

## Interplay between Thermodynamics and Kinetics in the Capping of InAs/GaAs(001) Quantum Dots

G. Costantini,<sup>†</sup> A. Rastelli, C. Manzano,<sup>\*</sup> P. Acosta-Diaz, R. Songmuang, G. Katsaros, O. G. Schmidt, and K. Kern

*Max-Planck-Institut für Festkörperforschung, Heisenbergstrasse 1, D-70569 Stuttgart, Germany*

(Received 30 March 2006; published 8 June 2006)

A microscopic picture for the GaAs overgrowth of self-organized InAs/GaAs(001) quantum dots is developed. Scanning tunneling microscopy measurements reveal two capping regimes: the first being characterized by a dot shrinking and a backward pyramid-to-dome shape transition. This regime is governed by fast dynamics resulting in island morphologies close to thermodynamic equilibrium. The second regime is marked by a true overgrowth and is controlled by kinetically limited surface diffusion processes. A simple model is developed to describe the observed structural changes which are rationalized in terms of energetic minimization driven by lattice mismatch and alloying.

DOI: [10.1103/PhysRevLett.96.226106](https://doi.org/10.1103/PhysRevLett.96.226106)

PACS numbers: 68.65.Hb, 68.37.Ef, 68.47.Fg

Quantum dots (QDs) are systems where the charge carriers are confined in three dimensions within a region smaller than their de Broglie wavelength. In the case of semiconductors, a promising route for their realization is represented by the three dimensional (3D) islands that spontaneously form during the initial phases of heteroepitaxial growth of lattice mismatched materials [1]. In principle, the required 3D confinement is directly obtained if the band gap of the epilayer material is smaller than that of the substrate. Nevertheless, freestanding islands are hardly ever employed but are instead covered by a capping layer (typically of the same material as the substrate) that preserves them from the external environment and suppresses nonradiative recombination through surface states also at the upper interface.

A fundamental aspect that has recently attracted substantial attention is that the deposition of a capping layer might be, and very often is, far from being harmless for the 3D islands. In fact, the capping procedure itself is a lattice mismatched heteroepitaxial process and is therefore associated with strain release, segregation, faceting, intermixing, strain-enhanced diffusion, etc. These phenomena take place at the island surface and can strongly modify the quantum dot morphology and composition. Since the optical and electronic properties of QDs strongly depend on their size, shape, and stoichiometry, a detailed microscopic understanding of the capping process that ultimately allows a tailoring of the optoelectronic characteristics becomes essential.

For the Ge/Si(001) system a microscopic picture of the dot overgrowth has recently been established [2,3]. The transformations that dome islands undergo while being capped by a Si layer have been precisely characterized and described based upon the dependence of the optimal island shape on its composition [3]. This is not the case for InAs/GaAs(001), the model system which is mostly used for QDs for optical investigations. Although several reports have been published on this topic [4–8], a coherent picture of the capping process based on a systematic microscopic

investigation is still lacking. In this Letter, ultrahigh vacuum scanning tunneling microscopy (UHV STM) is used for studying the GaAs overgrowth of well-characterized InAs QDs on GaAs(001). A detailed investigation as a function of the cap thickness and growth rate reveals the existence of two successive evolution regimes. Moreover, striking similarities with the SiGe case are found for the initial stages of the overgrowth, allowing us to identify general microscopic mechanisms responsible for the QD evolution during capping.

GaAs(001) wafers were prepared in a molecular beam epitaxy apparatus by deoxidation in UHV and subsequent growth of a 400 nm thick GaAs buffer layer at 610 °C. 1.8 monolayers (MLs) of InAs were then deposited at 500 °C [calibrated with the help of the  $(2 \times 4) \rightarrow c(4 \times 4)$  transition of the surface reconstruction] with a deposition rate of 0.008 ML/s and an  $As_4$  beam equivalent pressure of  $8 \times 10^{-6}$  mbar. This resulted in the self-organized formation of two coexisting types of islands: large multifaceted domes (height  $\sim 13$  nm) and smaller shallow pyramids (height  $\sim 2$  nm) [9,10]. In order to avoid In desorption, the sample temperature was lowered to 460 °C right after InAs growth and GaAs capping layers of various thickness (0–15 ML) were deposited at three different rates  $\Phi = 0.08, 0.6, \text{ and } 1.2$  ML/s. Subsequently, the sample heating was turned off resulting in an initial cooling rate of about 1 °C/s. As soon as room temperature was reached, the sample was transferred under UHV to an STM operated at room temperature.

Figures 1(a)–1(f) show the evolution undergone by InAs domes when capped with increasing amounts of GaAs at a rate of 0.08 ML/s. Even at the very first stages of capping (1 ML), strong modifications take place in the island morphology: the height is considerably reduced and a rim of material starts to accumulate around the island base [Fig. 1(b)]. After depositing 3 ML of GaAs, only a small part of the original island is still visible, while the surrounding rim increases its height and elongates in the  $[1 \bar{1} 0]$  direction of the substrate [Fig. 1(c)]. Further depo-

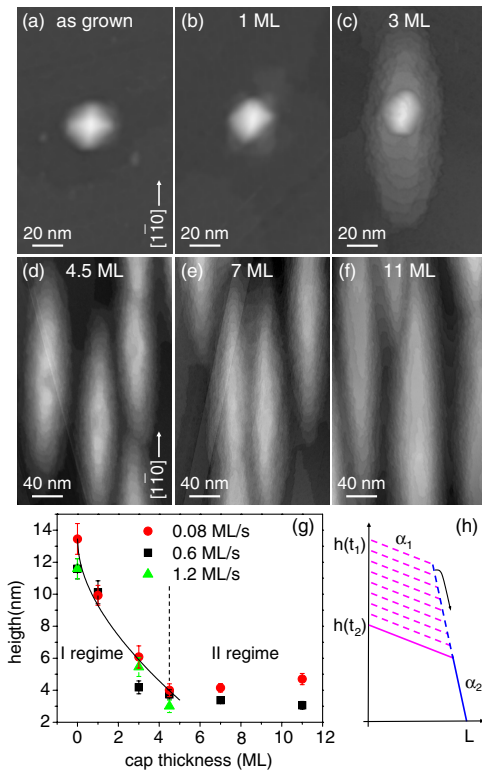


FIG. 1 (color online). (a), (b), (c), (d), (e), (f) STM images of InAs dome islands during GaAs capping at 0.08 ML/s. The gray scale has been adjusted independently for each image in order to enhance the morphological details. (g) Island height  $h$  as a function of the cap thickness for different GaAs deposition rates. The series at 0.08 ML/s was analyzed by STM, those at 0.6 and 1.2 ML/s by AFM. The solid line corresponds to the model's best fit (see text). (h) Schematic representation of the island shrinking.

sition of GaAs causes the complete disappearance of the faceted regions and a steady increase in the length of the elongated structures that eventually tend to merge [Figs. 1(d)–1(f)].

We measured similar evolution series for different GaAs deposition rates by *ex situ* atomic force microscopy (AFM). The quantitative analysis of the height of the overgrown structures is reported in Fig. 1(g). The most evident result is that two well-defined capping regimes exist. The first is characterized by a rapid height collapse of the pristine islands, while the second is marked by a true overgrowth of the remaining structures, as demonstrated by a non-negative slope of the height vs cap thickness. Comparable trends have been reported for the overgrowth of InAs islands under different experimental conditions [6,11]. A similar behavior has also been observed in the capping of Ge islands with Si [3], indicating the generality of the phenomenon. In the following, we will separately discuss the two regimes and identify the microscopic processes that govern the corresponding morphological transformations.

Higher resolution STM images of the first capping regime are reported in Fig. 2 for the central part of the actual

structure, i.e., disregarding the  $[1\bar{1}0]$ -elongated rim. The gray scale is related to the local surface slope, so that extended light or dark regions correspond to shallow or steep facets, respectively. A quantitative analysis of the facet distribution can be performed by a histogram representation of the surface gradient [12], in which island facets are displayed as spots [Figs. 2(e)–2(h)]. The pristine domes [Figs. 2(a) and 2(e)] are delimited by steep  $\{101\}$  and  $\{111\}$  as well as by shallow  $\{137\}$  facets [9,10]. After 1 ML of GaAs has been deposited [Fig. 2(b)], the  $\{137\}$  facets located at the islands' apex become larger while the other facets drastically reduce in size [see change in relative spot intensity in Fig. 2(f)]. With increasing cap thickness, the island shape further changes first into a pyramid dominated by  $\{137\}$  facets [2 ML GaAs, Figs. 2(c) and 2(g)] and finally into a truncated pyramid with an extended  $\{001\}$  top facet [3 ML GaAs, Figs. 2(d) and 2(h)]. This morphological transformation is quite similar to that occurring during the Si overgrowth of Ge domes [3] and is essentially the reverse of the pyramid-to-dome transition occurring during growth [13–15]. We notice that the temperature quenching rate of our experimental setup seems to be sufficient for preserving the overgrown structures when starting from a substrate temperature of 460 °C. In contrast to what was reported for 500 °C [8], we do not observe any relevant island leveling. Substantial changes in the island height can only be detected by intentionally introducing an extended annealing after a partial capping of the island.

Since relevant structural modifications happen already at the very first stages of the overgrowth (e.g., the deposition of only 0.28 nm GaAs—1 ML—induces an island height decrease of  $\sim 3$  nm, i.e., about 25% of the original value) a dynamic picture that accounts for the atomic-level processes occurring *during* the cap deposition is more suited than a static one based on thermodynamic arguments only [3,16,17]. The Ga atoms that are deposited directly onto the domes do not find favorable adsorption sites [18] since the lattice parameter of these islands approaches that of pure InAs across their tops [19,20]. As a consequence, Ga

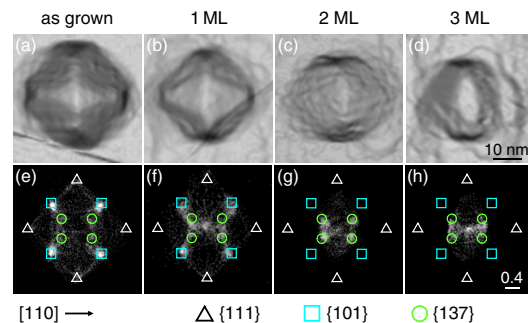


FIG. 2 (color online). Island shape evolution during the first capping regime. (a) Initial dome; (b) 1 ML, transition dome; (c) 2 ML, pyramid; (d) 3 ML, truncated pyramid. The gray scale of the STM topographies represents the local surface slope. (e), (f), (g), (h) Corresponding histograms of the 2D local surface gradient.

atoms tend to migrate away from the islands' apex and to accumulate at their base [Fig. 3(a)] where the lattice parameter is closer to GaAs. These Ga-rich regions represent advantageous alloying sites for the In atoms of the islands, whose chemical potential can decrease because of both entropy gain and strain energy release [21]. The net result is thus a redistribution of the islands' material from the top to the base that causes the observed height decay [Fig. 3(b)]. At the temperatures used during our experiments a bulk reshuffling of the atoms is kinetically hindered and the displacement of the island In-rich material can be produced by surface diffusion processes only. In other words, the lowering of the islands' height happens through a layer-by-layer removal of material, naturally producing an extension of the {137} facets at the expense of the steeper {101} and {111} ones [see Figs. 2, 1(h), and 3(b)]. This is the opposite of what happens during growth, where pyramids evolve into domes by layer-by-layer stacking of incomplete shallow facets at their tops [13–15]. From this point of view it is thus not surprising that a reverse dome-to-pyramid transition is associated with the island height decrease during capping.

Figure 1(g) clearly shows that for a cap thickness  $\leq 4$  ML the island decay is almost independent of the Ga deposition rate, indicating that this first overgrowth regime must be governed by rapidly occurring diffusion processes. This is coherent with the above microscopic description where the morphological transformations are induced by strong driving forces such as the release of elastic strain energy through alloying and the reduction of surface energy. In other words, this first regime is thermodynamically driven as further indicated by the island morphologies in Fig. 2 that closely resemble InAs/GaAs(001) equilibrium island shapes [13].

A simple 1 + 1D analytical model can be developed for describing the experimentally observed behavior. According to our previous analysis, the first capping regime can be schematically described as the island shrinking depicted in Fig. 1(h). As a consequence, the island volume can be expressed as  $V(t) = V_0 - \frac{[h_0 - h(t)]^2}{\alpha_2 - \alpha_1}$ , where

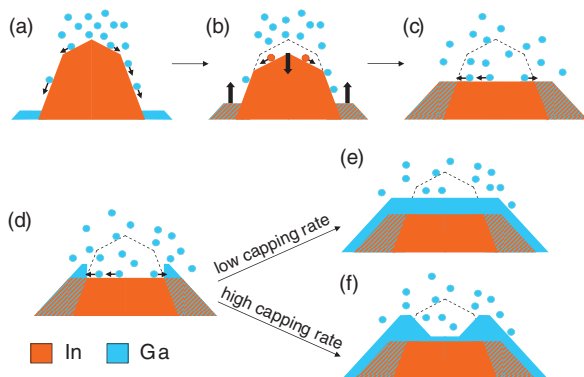


FIG. 3 (color). Schematic representation of the QD overgrowth process. Only the III-group elements are considered for simplicity.

$V_0$  and  $h_0$  are the initial island volume and height, respectively, and  $\alpha_1$  and  $\alpha_2$  are the slopes of the shallow and steep facets, respectively. The number of atoms that leave the island per unit time is thus  $\frac{dN_{\text{In}}}{dt} = -\Omega^{-1} \frac{dV}{dt}$ ,  $\Omega$  being the atomic volume. If we suppose that each new Ga atom arriving from the flux induces the detachment of  $\beta$  In atoms from the island, we find that  $\frac{dN_{\text{In}}}{dt} = \beta \frac{dN_{\text{Ga}}}{dt} = \beta \Phi 2L$ , where  $\Phi$  is the Ga flux and  $2L$  the lateral island size. This leads to a differential equation for the island height with a solution  $h(t) = h_0 - \sqrt{2C\Phi t}$ , where  $C = \beta \Omega L (\alpha_2 - \alpha_1)$ . Despite the extremely simplified assumptions of the model, this functional dependence describes quite well the initial rapid island shrinking and particularly its independence of the Ga deposition rate [Fig. 1(g)]. By fitting the model to the experimental data, we obtain  $\beta \sim 1$  which is a quite reasonable value indicating that, on average, each Ga atom reaching the island produces the outdiffusion of one In atom.

In contrast to the SiGe case [3], the alloy composed of the In from the island's top and the Ga of the capping flux is not incorporated into a faceted base, but accumulates into (001)-stepped flanks [Figs. 1(b)–1(f)]. The highly anisotropic reconstruction of the InGaAs(001) surface [22] is at the origin of the elongated island shapes [23] since, once adatoms have reached the island's base, they move preferentially along the  $[1\bar{1}0]$  direction [24]. Moreover, the adatom diffusion on these (001) stepped mounds has to be much slower than on the island's facets. In fact, contrary to the island height, the lateral extension of the flanks is kinetically determined, being larger for lower GaAs deposition rates [Figs. 4(a), 4(b), 4(d), and 4(e)].

While the height of the islands decreases with the amount of the deposited GaAs, that of the lateral flanks increases [Fig. 3(b)]. A closer look at the structures that develop just after these two opposite moving fronts have met reveals the formation of two shallow humps symmetrically located with respect to the original island position [Figs. 4(b), 4(e), and 3(d)]. These are caused by the same microscopic processes that induce the island shrinking. In this case, since the central part of the island is no more protruding, the preferential  $[1\bar{1}0]$  migration of Ga and In atoms away from its center (driven by lattice mismatch and alloying, respectively) leads to the formation of a central depression and of the observed lateral humps. We notice, however, that the In outdiffusion cannot go on indefinitely. In fact, even before capping, nominally pure InAs islands are actually characterized by a vertical compositional gradient [20,25–27], with a Ga content close to their base that can be even larger than 60% [19]. As a result, the driving mechanisms of In outdiffusion and alloying first weaken and then completely vanish with decreasing island height. Thereafter a true overgrowth sets in. A direct consequence of this effect can be found in the experiments by Songmuang *et al.* [7], where the height at which the island collapse stops scales with the indium percentage  $x$  of the  $\text{In}_x\text{Ga}_{1-x}\text{As}$  capping layer.

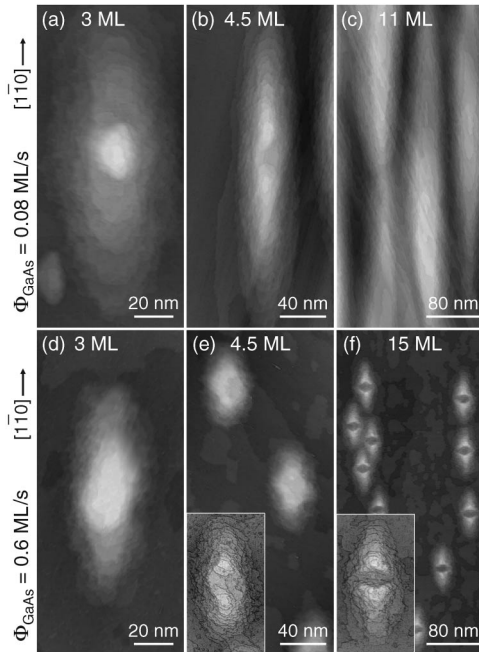


FIG. 4. Dependence of the overgrowth morphology on the GaAs deposition rate: upper row 0.08 ML/s, lower row 0.6 ML/s. (a) and (d) first regime; (b) and (e) transition between the regimes; (e) and (f) second regime. The contrast of the  $60 \times 100 \text{ nm}^2$  insets in (e) and (f) is enhanced by a derivative filtering.

At variance with what happens in the first capping regime [Figs. 4(a) and 4(d)], the morphological transformations occurring after the In outdiffusion has stopped strongly depend on the cap deposition rate [Figs. 4(c) and 4(f)]. At a GaAs rate of 0.08 ML/s the humps in Fig. 4(b) are quickly smoothed out and only  $[1\bar{1}0]$  elongated mounds remain, centered at the position of the original islands [Figs. 4(c) and 3(e)]. On the contrary, when GaAs is deposited at 0.6 ML/s, the two protrusions continue developing and evolve first into camel humpback structures [7,28] [Figs. 4(f) and 3(f)] and eventually into rhombus-shaped structures with a central hole [29]. For both deposition rates, a  $c(4 \times 4)$  surface reconstruction indicates a pure GaAs growing front for cap thicknesses larger than 15 ML. The morphological evolution during this second capping regime is mainly driven by a migration of Ga adatoms away from the position of the embedded island that acts as a stressor and causes a local lattice expansion [18]. As already noticed, this preferential  $[1\bar{1}0]$  diffusion over stepped (001) terraces is evidently slower than the diffusion processes governing the first capping regime. As a consequence, at lower deposition rates, longer diffusion lengths allow a surface smoothing. On the contrary, at higher rates the ability of surface diffusion to minimize surface curvature is kinetically reduced and the ridged morphology is reproduced for higher cap thicknesses. It has been recently reported that if the Ga deposition occurs under  $\text{As}_2$  instead of  $\text{As}_4$  flux, the anisotropy between the migration distances along  $[1\bar{1}0]$  and  $[110]$  is

significantly reduced and rounded ring-shaped structures form instead of the camel humpbacks [28]. We believe that the same type of microscopic processes described here are responsible also for the ring formation.

In conclusion, we have thoroughly analyzed the GaAs overgrowth of InAs self-organized islands and determined the existence of two capping regimes. The first is characterized by a substantial island shrinking almost independent of the cap deposition rate. The resulting island structures closely resemble thermodynamic equilibrium shapes. The second is marked by a true overgrowth and is essentially determined by a kinetically limited diffusion on a stepped (001) surface. Depending on the GaAs rate, elongated mounds or structures with a central hole are formed. A simple description of the observed phenomenology has been developed based on microscopic diffusion processes. This model coherently accounts for many experimental reports on semiconductor island capping reported in the literature.

\*Present address: Institut für Experimentelle und Angewandte Physik, Christian-Albrechts-Universität zu Kiel, D-24098 Kiel, Germany.

†Electronic address: gio@fkf.mpg.de

- [1] D. Bimberg, M. Grundmann, and N. N. Ledentsov, *Quantum Dot Heterostructures* (John Wiley & Sons, Chichester, 1999).
- [2] P. Sutter and M. G. Lagally, *Phys. Rev. Lett.* **81**, 3471 (1998).
- [3] A. Rastelli *et al.*, *Phys. Rev. Lett.* **87**, 256101 (2001).
- [4] J. M. Garcia *et al.*, *Appl. Phys. Lett.* **71**, 2014 (1997).
- [5] K. Takehana *et al.*, *J. Cryst. Growth* **251**, 155 (2003).
- [6] P. B. Joyce *et al.*, *Appl. Phys. Lett.* **79**, 3615 (2001).
- [7] R. Songmuang *et al.*, *J. Cryst. Growth* **249**, 416 (2003).
- [8] Q. Gong *et al.*, *Appl. Phys. Lett.* **85**, 5697 (2004).
- [9] G. Costantini *et al.*, *Appl. Phys. Lett.* **85**, 5673 (2004).
- [10] G. Costantini *et al.*, *J. Cryst. Growth* **278**, 38 (2005).
- [11] F. Ferdos *et al.*, *Appl. Phys. Lett.* **81**, 1195 (2002).
- [12] A. Rastelli and H. von Känel, *Surf. Sci.* **515**, L493 (2002).
- [13] P. Kratzer *et al.*, *Phys. Rev. B* **73**, 205347 (2006).
- [14] M. C. Xu *et al.*, *J. Appl. Phys.* **98**, 083525 (2005).
- [15] F. Montalenti *et al.*, *Phys. Rev. Lett.* **93**, 216102 (2004).
- [16] R. Blosser and A. Lorke, *Phys. Rev. E* **65**, 021603 (2002).
- [17] L. G. Wang *et al.*, *Appl. Phys. A* **73**, 161 (2001).
- [18] Q. H. Xie *et al.*, *Appl. Phys. Lett.* **65**, 2051 (1994).
- [19] R. Kegel *et al.*, *Phys. Rev. B* **63**, 035318 (2001).
- [20] B. Krause *et al.*, *Phys. Rev. B* **72**, 085339 (2005).
- [21] U. Denker *et al.*, *Phys. Rev. Lett.* **94**, 216103 (2005).
- [22] J. G. Belk *et al.*, *Surf. Sci.* **387**, 213 (1997).
- [23] Z. M. Wang *et al.*, *J. Appl. Phys.* **96**, 6908 (2004).
- [24] E. Penev *et al.*, *Phys. Rev. B* **69**, 115335 (2004).
- [25] N. Liu *et al.*, *Phys. Rev. Lett.* **84**, 334 (2000).
- [26] A. Lenz *et al.*, *Appl. Phys. Lett.* **81**, 5150 (2002).
- [27] D. M. Bruls *et al.*, *Appl. Phys. Lett.* **81**, 1708 (2002).
- [28] D. Granados and J. M. Garcia, *Appl. Phys. Lett.* **82**, 2401 (2003).
- [29] H. Heidemeyer *et al.*, *Appl. Phys. Lett.* **80**, 1544 (2002).